Synthetic Diversity To Mitigate Out-of-Band Interference in Widely Tunable Wireless Receivers

Alyosha Molnar
School of Electrical and Computer Engineering
Cornell University
Ithaca, NY, USA
am699@cornell.edu

Zachariah Boynton
School of Electrical and Computer Engineering
Cornell University
Ithaca, NY, USA
zgb4@cornell.edu

Sweta Soni
School of Electrical and Computer Engineering
Cornell University
Ithaca, NY, USA
ss3964@cornell.edu

Sanaz Sadeghi
School of Electrical and Computer Engineering
Cornell University
Ithaca, NY, USA
ss3842@cornell.edu

***Abstract*— Here we present a combined RF hardware/DSP technique to synthesize effective channel diversity in single-antenna wireless systems. This allows digital suppression of out-of-band interference artifacts in widely tunable wireless receivers with one or more antennas, including artifacts from LO phase noise. A passive inductor-capacitor (LC) network provides gain and phase diversity between channels and across frequency. Since amplitude and phase of in-band artifacts are set by the amplitude and phase of the out-of-band interference that generates them, they can be suppressed in DSP without knowledge about the interferer itself. The feasibility of this approach is demonstrated mathematically, with numerical system simulations, and full circuit simulation.**

Keywords—Software defined radio, interference mitigation, receiver, phase noise

I. Introduction

A long-standing goal in wireless communications has been to develop highly flexible radios, able to tune across a wide frequency range while being resilient to interference. This goal is increasingly urgent as the RF spectrum has become ever more cluttered. Frequency flexibility allows radios to dynamically access available spectrum while dodging interferers. Active circuitry to support multi-octave frequency tuning in receivers has proven straightforward, accomplished simply by tuning the local oscillator (LO) through a combination of octave-tunable oscillators and programmable frequency dividers. Furthermore, receiver sensitivity can be maintained across this tuning range if a sufficiently wide-band antenna is used [1,2] simply by implementing a wide-band low-noise amplifier and mixer. However, the utility of widely tunable radio receivers has been limited by their relatively high susceptibility to out-of-band (OOB) interference. Thus, interference tolerance has been an important focus in the development of widely tunable radio receivers. Here we present a receiver architecture, combining a novel hardware approach with appropriate signal processing, to allow both wide tuning and enhanced tolerance to strong OOB interferers.

This work was supported in part by the Semiconductor Research Corporation (SRC) and DARPA, as well as by NSF grant number 1641100.

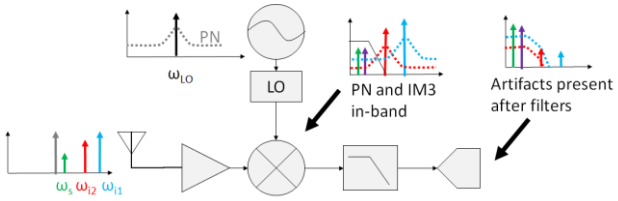

Figure 1. Illustration of in-band artifacts from out-of-band interferers. Arrows represent narrow band signals: green: wanted; red, blue: OOB interferers. Purple: IM3, dotted lines: reciprocally mixed phase noise.

Out-of-band interferers can degrade one's desired signal through two primary mechanisms. The first is through circuit nonlinearity, typically in front-end amplifiers and mixers. Interference plus nonlinearity can result in cross compression, where an OOB interferer causes the wanted signal to lose gain. Nonlinearity can also cause intermodulation, when pairs of OOB interferers generate in-band 3rd-order intermodulation (IM3) products. The second general mechanism by which OOB interference degrades in-band signal sensitivity, is through reciprocal mixing of spectral impurities in the LO. This can be caused by spurious tones in the LO, or as a result of phase noise. These effects are summarized in Fig. 1.

Narrowly-tunable receiver front ends mitigate these effects with a linear high-Q band-pass filter (BPF). The BPF rejects any interferers outside the desired receive band before they can generate in-band artifacts. In a widely tunable receiver the front-end BPF must accommodate the receiver's entire tuning range, leaving it open to any strong interferers in that band. Approaches employing tunable BPF or banks of BPF can be used, but come with significantly greater complexity and/or increased in-band loss, and still provide only limited flexibility. Meanwhile, advances in RF circuits using linear-time-varying techniques have provided receivers with much higher out-of-band linearity [3,4], but have not provided concomitant reductions in phase noise, which remains limited by fundamental noise-power trade-offs in the LO itself [5]. The goal of the work presented here is to provide an alternate technique for suppressing interference artifacts in a widely tunable receiver without requiring real-time tuning of the RF front-end.

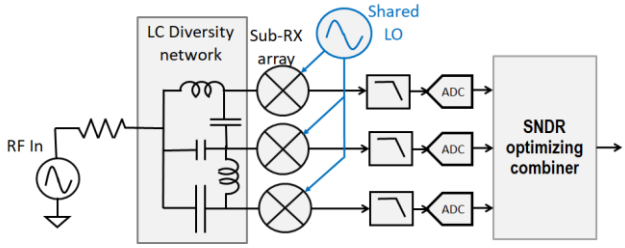

Figure 2. Proposed receiver architecture

II. Synthetic Diversity Concept

A. Core Concept

The core idea of this work is to adopt the concept of channel diversity to distinguish between signal and interference artifacts, but with only one RF port (antenna), as shown in Fig. 2. Diversity is generated with a passive, low loss circuit such as an inductor-capacitor (LC) network with a single input and N output taps. This yields a length-N vector of transfer functions from input to outputs $\overrightarrow{H(j\omega)}$ which feed N sub-receivers, which share a single LO. The sub-receivers outputs are digitized and optimally complex weighted and summed in the digital domain. Since the outputs of these receivers will be added coherently after digitization, the SNR of each sub-receiver can be N times worse without loss of overall SNR. This in turn means each sub receiver can be operated at a DC power lower by at a factor of N.

B. Basic Mathematical Formulation

The receiver sees signal (v_s) and interference (v_i) with distinct center frequencies, ω_s and ω_i, respectively. Passing through the LC diversity network, signal and interference acquire different complex gains $\overrightarrow{H(\omega)}$ at each sub-receiver, resulting in voltages describable as a length-N vector of

$$\overrightarrow{v_{RX}} = v_s\overrightarrow{H(j\omega_s)} + v_i\overrightarrow{H(j\omega_i)} \tag{1}$$

The OOB interferers in each sub-receiver generate in-band artifacts as in Fig. 1, but these artifacts inherit their relative phase and gain from the interferers themselves [6], as illustrated in Fig. 3. Reciprocal mixing artifacts take the form

$$\overrightarrow{v_n} = PN(\omega_i - \omega_{LO})v_i\overrightarrow{H(j\omega_i)} \tag{2}$$

where $PN(\Delta\omega)$ is the phase noise of the shared LO at frequency offset $\Delta\omega = |\omega_i - \omega_{LO}|$. Similarly, IM3 generation will take the form

$$\overrightarrow{v_{\Im 3}} = a_3 v_{i1} {v_{i2}}^2 \overrightarrow{H(j\omega_{i1})|H(j\omega_{i2})|^2} \tag{3}$$

where $v_{i1}, v_{i2}, \omega_{i1}$, and ω_{i2},are the complex amplitudes and center frequencies of two OOB interferers, and a_3 is the 3rd order power-series coefficient. As shown in Fig. 3, for phase noise, while OOB interferers are suppressed after down-conversion by analog low-pass filters (LPF), in-band artifacts are not, such that

$$\overrightarrow{v_{out}} = v_s\overrightarrow{H(j\omega_s)} + PN(\omega_i - \omega_{LO})v_i\overrightarrow{H(j\omega_i)} \tag{4}$$

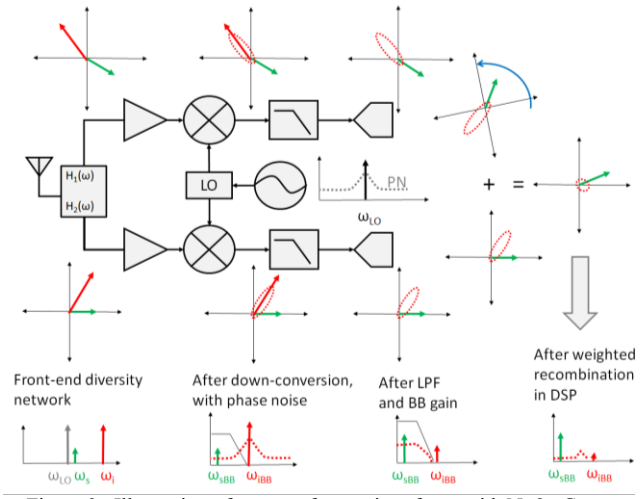

Figure 3. Illustration of concept for one interferer, with N=2. Green arrows represent complex weights of wanted signal, Red arrows represent the interferer which is suppressed by LPF. Dashed ovals represent reciprocally mixed PN, which is in-band but can be suppressed after digitization with appropriate complex weighting. Bottom row shows corresponding power spectra.

By generating N distinct versions of both signal and interference artifacts, it is possible to recombine the signals after digitization with a complex weight vector, $\vec{W}$. $\vec{W}$ can be chosen to maximize SNR of signal, $v_s\left|\vec{W}\cdot\overrightarrow{H(j\omega_s)}\right|$, as well as to minimize the magnitude of artifacts $\left|\vec{W}\cdot\overrightarrow{v_n}\right|$, $\left|\vec{W}\cdot\overrightarrow{v_{\Im 3}}\right|$. In the absence of interference, SNR is optimized when $\vec{W} = \overrightarrow{H^*(j\omega_s)}$, equivalent to a matched filter, while artifacts are minimized by setting $\vec{W} \perp \overrightarrow{v_n}$. Which is equivalent to $\vec{W} \perp \overrightarrow{H(j\omega_i)}$. Optimal noise while nulling interference artifacts can be achieved by setting

$$\vec{W} = \overrightarrow{H^*(j\omega_s)} - \frac{\overrightarrow{H^*(j\omega_s)}\overrightarrow{H(j\omega_i)}}{\overrightarrow{H^*(j\omega_i)}\overrightarrow{H(j\omega_i)}}\overrightarrow{H^*(j\omega_i)} \tag{5}$$

C. Key Constraints on LC Network

The mathematics of the previous section do not dictate a specific front-end LC network, but certain properties of the network do directly impact performance. While interference artifacts can be suppressed relative to the signal for any $\overrightarrow{H(j\omega_i)} \neq \overrightarrow{H(j\omega_s)}$, noise figure can be significantly degraded if $\overrightarrow{H(j\omega_i)}$ and $\overrightarrow{H(j\omega_s)}$ are too similar. Specifically, if $\vec{W}$ is chosen to maximize signal and null interference artifacts as in (5), then noise figure will be approximately:

$$NF = 10log\left(1 + \frac{\frac{v_{nRX}^2}{4kTR_S}}{\left\|\overrightarrow{H(j\omega_S)}\right\|_2^2 - \frac{\left|\overrightarrow{H^*(j\omega_S)}\overrightarrow{H(j\omega_i)}\right|^2}{\left\|\overrightarrow{H(j\omega_i)}\right\|_2^2}}\right) \tag{6}$$

Where v_{nRX}^2 is the input-referred noise of a single sub-receiver.

Thus, the front-end network should be optimized to maximize in-band gain, $\left\|\overrightarrow{H(j\omega_s)}\right\|_2^2$ across all possible ω_s. Additionally, the inner product of the signal and interferers' transfer functions, $\left|\overrightarrow{H^*(j\omega_s)}\overrightarrow{H(j\omega_i)}\right|$ should be minimized so that the interferer can be nulled without significantly reducing signal gain. Interestingly even when $\vec{W}$ is chosen as a matched filter, so as to maximize SNR in the absence of interference, interference artifacts will still be subject to attenuation proportional to the inner product $\left|\overrightarrow{H^*(j\omega_s)}\overrightarrow{H(j\omega_i)}\right|$, providing suppression of moderate and weak interference artifacts. Thus, optimizing the front-end network to allow nulling of interference artifacts with high SNR also intrinsically suppresses (though does not fully null) the artifacts when they are not actively nulled.

III. LC Network Design and Simulation Results

A. LC network optimization

In order to explore what kind of networks meet the requirements from section II.c., we looked at a variety of LC networks. We optimized LC choices by minimizing a weighted sum of: a) Baseline NF when no interferer is present, averaged across the ω_s frequency range: 1-2GHz; b) NF when interferer is present at ω_i and nulled, averaged across both ω_s, ω_i swept over 1-2GHz; c) Total inductance and capacitance, including both number and value of components. Components were modelled with realistic quality factor (Q) and self-resonant frequencies (SRF).

For the resulting non-convex optimization, we used an evolutionary algorithm, starting with either a random or known topology. We used a combination of gradient descent, and semi-random testing of permutations in inductor placement. keeping only permutations that, once re-optimized through gradient descent, provided better results. This optimization found many different LC topologies with similar performance. Two example networks for N=4, are shown in Fig. 4 with associated complex transfer functions, $\overrightarrow{H(\omega)}$. Unsurprisingly, all optimized topologies' transfer functions shared certain properties, including roughly constant summed amplitude across the optimization frequency range, and rapid changesin the relative magnitude and phase of different sub-channels with changing frequency. Critically, this was true even where the initial network was a known topology, such as an artificial transmission line or bank of BPF, but in all cases evolved away to other non-standard, but better-performing topologies.

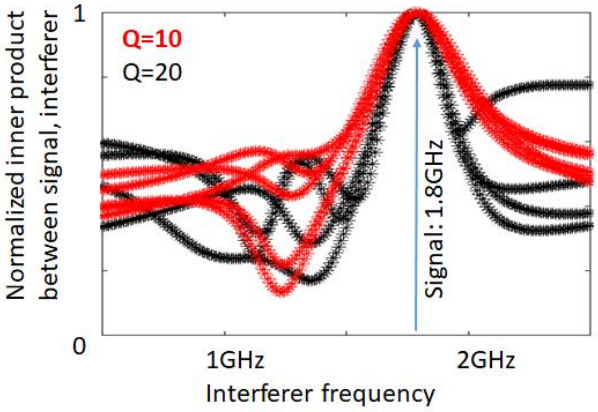

Figure 5. Signal-interferer inner product vs Interferer frequency for multiple evolved LC networks with two values of inductor Q.

Networks with higher-Q components tend to provide better performance. This is in part because they result in lower loss for the wanted signal, leading to a better baseline NF. Higher Q components also help because they provide higher-Q resonances, leading to sharper fluctuations in amplitude and phase across frequency. Sharper fluctuations in $\overrightarrow{H(\omega)}$ allow interference and signal transfer functions to diverge at smaller frequency offsets, reducing their inner product more quickly, as shown in Fig. 5. Networks with larger numbers of taps, N, can, in principal, also provide greater diversity at a cost in component count. Simulations show networks with greater numbers of taps provided better performance, up to about 5 taps. Beyond a certain number of taps the evolutionary algorithm optimizes component cost by shorting pairs taps together, providing no additional diversity. Preliminary studies of networks optimized for more than one simultaneous interferer show greater benefits to having more taps, but further study is needed to fully understand this optimization space.

B. Simulations in Time Domain

The analysis in sections II and III.B were performed primarily in the frequency domain. In order to confirm that the proposed concept works on realistic noise and signals, we also performed time-domain simulations. We modelled both signal and interferer as QPSK-modulated sinusoids, with the interferer 60dB stronger than the wanted signal. LC networks generated using the evolutionary approach described in section II.A. were simulated in the time domain with additive noise, and a physically reasonable time-domain model of down conversion

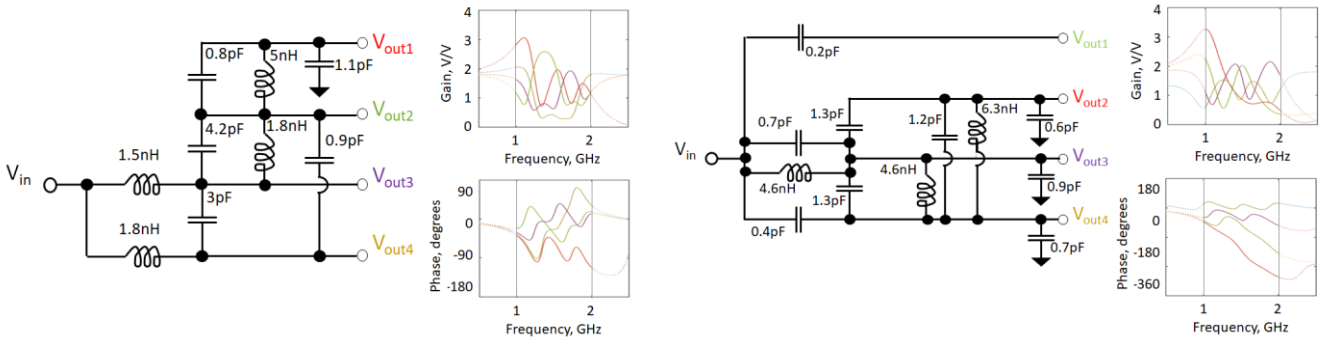

Figure 4. Two example evolved LC networks and associated complex transfer functions.

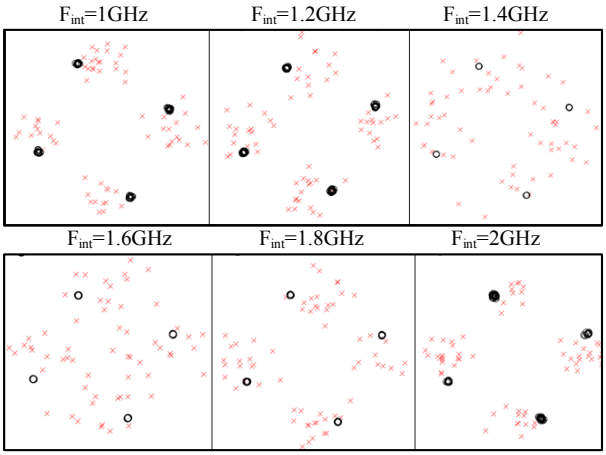

Figure 6. Constellations from temporal simulations for signal frequency=1.5GHz for various interferer frequencies. Red: receiver without LC network, black: with LC and associated weighting.

mixers, driven by a shared local oscillator with phase noise. As shown in Fig. 6, the model predicts significant degradation of the signal if a simple receiver without LC network and associated weighting is used. When synthetic diversity is included, these phase noise artifacts are suppressed, improving the RMS error vector magnitude (EVM) by more than 20dB.

These simulations, however, revealed an interesting caveat. The proposed approach works well to suppress reciprocal mixing of PN at a frequency offset of $|\omega_{LO} - \omega_i|$. However, one can also see reciprocal mixing from LO PN at offset $|\omega_{LO} + \omega_i|$ which is *not* suppressed by the same weight vector, and, indeed, requires a complex conjugate weight vector to suppress. This is similar to what was recently reported in certain distributed duplexing radios [7] (see Fig. 7). This 2nd noise mechanism can also be nulled, with an additional cost to noise figure. However, as the phase noise associated with this secondary mechanism is very far from the LO frequency itself, one can also just band limit the LO's noise (and so the LO itself) while still allowing a tuning range of F_{max}/F_{min}=3.

C. Expected Performance and Full Circuit Simulation

We investigated expected performance with realistic circuit element values (L<5nH, C<5pF, Q=10-20) for N=4, and networks optimized for 1GHz<f<2GHz. Compared to an equivalent receiver without an LC network and with all N sub-receivers combined coherently, we found baseline loss/NF

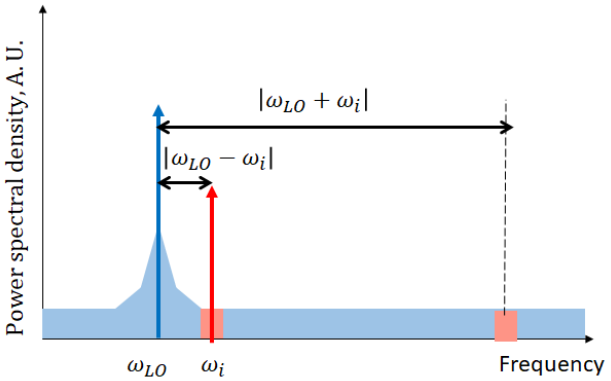

Figure 7. illustration of both frequencies where phase noise may reciprocally mix with a signal at ω_i.

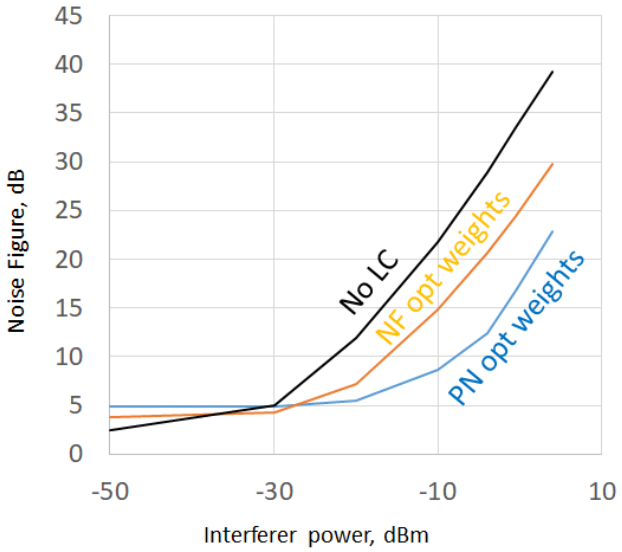

Figure 8. Plot of noise figure vs interference strength in full circuit simulations in Cadence, for three different configurations.

degradation to be < 1dB, and typical signal attenuation with interferers nulled to be <3dB. The optimized LC network also acted as impedance matching. Finally, no extra dc power would be needed in the active circuitry, since sub-receivers consume 1/N the dc power of the full system, and have a factor of N higher input referred noise for same overall NF.

We confirmed these results with full, transistor-level receiver circuit simulations in Cadence, for one of the evolved LC networks, and looked at NF, while sweeping interferer power, with band-limited PN on the LO. Fig. 8 shows the results for an LO frequency of 1.8GHz, interferer at 1.5GHz, and -140dBc/Hz phase noise. NF is shown for three configurations: a) LC as designed, baseband weights chosen for PN suppression; LC as designed, baseband weights chosen for best NF without interference and c) no LC, 4 channels shorted in parallel. As can be seen, with no LC, NF degrades quickly as the interferer increases in power. This is improved by the divergence between interferer and signal vectors with the LC network, and further improved by up to 15dB, when this divergence is exploited to null the phase noise artifact. Residual degradation is likely due to a combination of imperfect weights, wide-band noise, and second-order nonlinear phenomena.

IV. Automatic Interference Suppression

To be fully useful, the described approach must be combined with techniques to rapidly discover and suppress interference artifacts on the fly without *a priori* knowledge about the underlying interferer(s). We can assume we know the optimal weights for minimum NF *a priori,* since we know the wanted receive frequency and LC network topology. However, we *don't know* interference frequencies in advance, so interference artifacts and their transfer functions must be discovered in real time. Here we propose one algorithm as an approach to doing this.

A. Algorithm Setup

Start with the measured output as a time-series of N complex outputs, $\overrightarrow{v_{out}(t)}$, and assume $\overrightarrow{v_{out}(t)}$ is the sum of two other vectors as in (4):

$$\overrightarrow{v_{out}(t)} = \overrightarrow{H_s} \cdot v_s(t) + \overrightarrow{H_n} \cdot v_n(t) \quad (7)$$

Again, $v_s(t)$ is the underlying wanted signal , and $\overrightarrow{H_s}$ is its complex-valued transfer function vector. In the case of phase noise, the interference artifact $v_n(t)$ is equal to the interferer passed through its associated transfer function, $\overrightarrow{H_n} = \overrightarrow{H_\iota}$, and mixed against PN. $\overrightarrow{H_s}$ is known, because we know the signal frequency, we want to find $v_s(t)$.

B. Proposed algorithm:

Step 1: Isolate interference artifacts by extracting the part of $\overrightarrow{v_{out}(t)}$ orthogonal to $\overrightarrow{H_s}$, call this $\overrightarrow{v_{out\_\iota}(t)}$.

$$\overrightarrow{v_{out_\iota}(t)} = \overrightarrow{v_{out}(t)} - \overrightarrow{H_s}\frac{\overrightarrow{H_s}^* \overrightarrow{v_{out}(t)}}{\overrightarrow{H_s}^* \overrightarrow{H_s}}$$

$$= \overrightarrow{H_n} \cdot v_n(t) - \overrightarrow{H_s}\frac{\overrightarrow{H_s}^* \overrightarrow{H_n} \cdot v_n(t)}{\overrightarrow{H_s}^* \overrightarrow{H_s}} \quad (8)$$

Step 2: Perform principal component analysis on $\overrightarrow{v_{out\_\iota}(t)}$: the 1st principle component will be $\overrightarrow{H_n}\left[I - \frac{\overrightarrow{H_s}\overrightarrow{H_s}^*}{\overrightarrow{H_s}^* \overrightarrow{H_s}}\right]$, and the projection of $\overrightarrow{v_{out\_\iota}(t)}$ onto this component is $v_n(t)$. If multiple strong interferers are present, more principal components will be needed.

Step 3: Isolate $\overrightarrow{H_n}$ by finding the correlation between $\overrightarrow{v_{out}(t)}$, $v_n(t)$ across time, and assuming $v_s(t)$, $v_n(t)$ are uncorrelated.

$$\widehat{H_n} \propto \sum_t \overrightarrow{v_{out}(t)} v_n{}^*(t) = \sum_t \overrightarrow{H_s} \cdot v_s(t) v_n{}^*(t) + \overrightarrow{H_n}|v_n(t)|^2$$

$$= N\overrightarrow{H_n}\sigma_n^2 \quad (9)$$

Step 4: Compute optimal $\vec{W}$ as in [5] from $\overrightarrow{H_s}$ and $\widehat{H_n}$:

$$\vec{W} = \overrightarrow{H_s}^* - \widehat{H_n}^* \frac{\overrightarrow{H_s}^* \widehat{H_n}}{\widehat{H_n}^* \widehat{H_n}} \quad (10)$$

Step 5: Apply $\vec{W}$ to extract estimated signal $\widehat{v_s(t)}$:

$$\widehat{v_s(t)} = \overrightarrow{v_{out}(t)}\vec{W}$$

$$= \left(\left\|\overrightarrow{H_s}\right\|_2^2 - \frac{\left|\overrightarrow{H_s}^* \overrightarrow{H_n}\right|^2}{\left\|\overrightarrow{H_n}\right\|_2^2}\right) v_s(t) \quad (11)$$

C. Simulated results:

We tested this algorithm on data from simulations described in section III.B.. As can be seen in Fig. 9, the proposed algorithm succeeds in finding and suppressing phase noise artifacts from out-of-band interference, based only on measurements and knowledge of the signal transfer function.

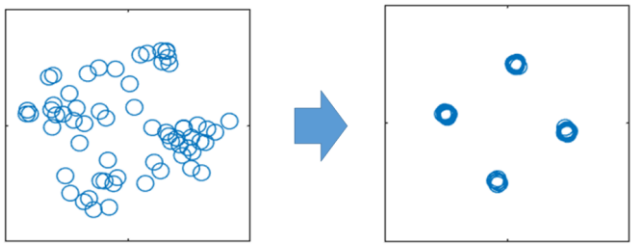

(a) (b)

Figure 8. Simulation results. a) Output using pure NF optimization where $\vec{W} = \overrightarrow{H^*(j\omega_s)}$ and b) Output from same data after using algorithm in section IV. B.

V. Conclusions

We have proposed a new receiver architecture that synthesizes diversity in a front-end passive network, and then uses it to suppress in-band artifacts from out-of-band interferers. Furthermore the proposed approach is shown to work for signals and interferers from a wide frequency range (~ 1 octave) and does not require *a priori* knowledge about any given interferer to suppress its artifacts. The proposed approach only provides strong suppression to artifacts from sparse (in spectrum) interference, while mild suppression of other interferers' artifacts does not require sparsity. Performance in suppressing close-in interferers' artifacts is limited by the Q of components in network, much as it would be in a more traditional BPF. Assuming sparsity in strong interferers is a reasonable assumption, and better close-in performance is likely possible using other styles of resonator than LC. Further work is needed to better understand how to optimize LC or other resonant networks, especially for multiple interferers, and for artifacts beyond phase noise, such as IM3. Nonetheless, this approach opens a new avenue for widely tunable interference-resistant wireless receivers.

Acknowledgment

The Authors would like to acknowledge the suggestions of Yorgos Palaskas and other ComSenTer Liaisons for their encouragement in developing this concept.

References

[1] L. Van der Perre, et al., "Architectures and Circuits for Software-Defined Radios: Scaling and Scalability for Low Cost and Low Energy," IEEE ISSCC. *Digest of Technical Papers*. vol. 50 San Francisco:, pp. 568 - 569, 2007

[2] J. Craninckx, et al. "A Fully Reconfigurable Software-Defined Radio Transceiver in 0.13um CMOS," in *IEEE ISSCC Digest of Technical Papers*. vol. 50 San Francisco, pp. 346 – 607 2007

[3] Borremans et. al. "A 40 nm CMOS 0.4 – 6 GHz Receiver Resilient to Out-of-Band Blockers" *IEEE JSSC*, vol. 46, no 7, 2011

[4] C. Andrews and A. C. Molnar, "A Passive Mixer-First Receiver With Digitally Controlled and Widely Tunable RF Interface," in *IEEE JSSC*, vol. 45, no. 12, pp. 2696-2708, 2010

[5] T. Tapen, Z. Boynton, et. al., "The Impact of LO Phase Noise in N-Path Filters", IEEE TCAS I, issue 99, pp 1-16, 2017

[6] S. Jacobsson et. al. "Massive MU-MIMO-OFDM Uplink with Hardware Impairments: Modeling and Analysis", 2018 52nd Asilomar Conference on Signals, Systems, and Computers

[7] T. Tapen, et. al., "An Integrated, Software-Defined FDD Transceiver: Distributed Duplexing Theory and Operation," in *IEEE Transactions on Circuits and Systems I: Regular Papers*, Nov 2019